Water Science & Technology

IWA PUBLISHING

Water Science & Technology Vol 84 No 4, 906 doi: 10.2166/wst.2021.275

Effect of the famine phase length on the properties of aerobic granular sludge treating greywater

U. Rojas-Z [a], C. Fajardo-O [a], I. Moreno-Andrade [b] and O. Monroy [a,*]

[a] Department of Biotechnology, Universidad Autónoma Metropolitana, Av. San Rafael Atlixco 186, Col. Vicentina, 09340 Iztapalapa, Mexico City, Mexico
[b] Laboratory for Research on Advanced Processes for Water Treatment, Engineering Institute, U. A. Juriquilla, Universidad Nacional Autónoma de México, Blvd Juriquilla 3001, 76230 Juriquilla, Qro, Mexico
*Corresponding author. E-mail: monroy@xanum.uam.mx

UR, 0000-0002-3672-5092; CF, 0000-0001-5259-956X; IM, 0000-0002-1400-7241; OM, 0000-0003-0073-711X

ABSTRACT

Sequencing batch reactors (SBR) treating high-strength greywater need an aerobic granular sludge (AGS) with good properties, such as a low sludge volume index (SVI) and high settling velocities and substrate uptake rates to yield short settling and aeration stages. To promote the formation of stable granular sludge, the length of the famine phase could be a key factor. In this regard, the effect of the duration of this variable on the AGS properties was assessed by comparing a gradual versus an abrupt reduction of the famine phase in two SBR treating greywater. The initial average famine phase of 3.3 h was gradually reduced to 0.3 h over 20 weeks in one reactor, and abruptly in another one. This condition induced filamentous outgrowth, as well as the deterioration on the properties of the sludge; the effect was more accelerated when the famine periods were abruptly shortened. In both cases the reduction on the famine periods induced increased organic loading rates, which led to degranulation events when it was higher than 2.5 g-chemical oxygen demand g-volatile suspended solids^{-1} d^{-1}. Afterwards, the biomass adapted to this situation, by forming new small-filamentous aggregates with similar SVI to that of the stable AGS formed with the longest famine period.

Key words: aerobic granules, famine phase, greywater, sequencing batch reactor, wastewater treatment

HIGHLIGHTS

- The reduction in the famine phase length induces filamentous overgrowth and the deterioration of the properties of AGS.
- Overstressed organic loading rates can lead to the biomass degranulation.
- Small-size filamentous aggregates can present a similar sludge volume index to that of the stable-AGS.
- A famine fraction of 0.55 with respect to the total cycle length is enough to ensure the stability of the AGS.

GRAPHICAL ABSTRACT

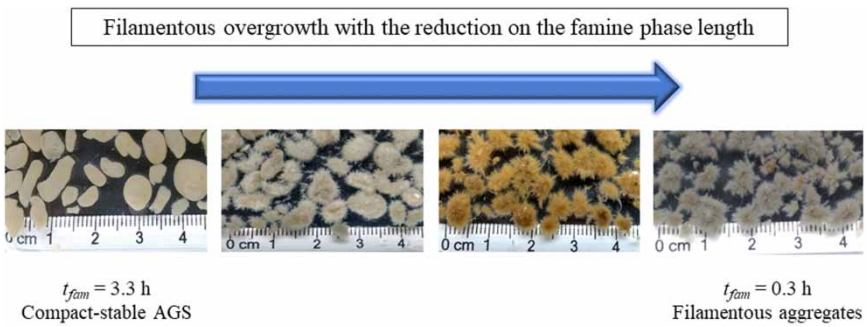

INTRODUCTION

The installation of decentralized greywater treatment systems to reclaim water for non-potable uses and nutrients, requires a set of low footprint and efficient technologies (Bajpai *et al.* 2019). Greywater can be efficiently treated by sequencing batch reactors (SBR) with aerobic granular sludge (AGS), which is a biofilm that presents remarkable properties, such as high density (κg) and settling velocity (v_s), low sludge volume index (SVI) and a structure which withstands toxics and organic shocks with high substrate (r_s) and oxygen uptake rates (OUR) (Sengar *et al.* 2018; Sharaf *et al.* 2019; Avila *et al.* 2021). These characteristics allow an efficient solid–liquid separation, as well as the application of high volumetric exchange ratios (V_{er}) and short aeration and settling stages; key parameters to reduce the hydraulic retention time (HRT). AGS has been applied for the treatment of different kinds of effluents, including petrochemical (Caluwé *et al.* 2017), swine (Wang *et al.* 2020), chemical industrial wastewater (Qi *et al.* 2020), and greywater (Rojas-Z *et al.* 2017) showing that it is a robust and flexible technology with a broad field of application. However, when aerobic granular systems are fed with complex wastewaters, containing slowly biodegradable pollutants in particulated form, the deterioration of the granular structure due to the growth of filamentous microorganisms has been observed (Pronk *et al.* 2015; Yuan *et al.* 2019).

Filamentous overgrowth in AGS is a negative aspect that affects the stability and the operational efficiency of the SBR, as it leads to the increase of the granules size, producing fluffy and bulky aggregates with poor settling properties and density, which can be easily washed out from the system (Sharaf *et al.* 2019). This phenomenon is produced by the adsorption and degradation of the particulated substrates at the surface of the granules during the aeration stage, leading to substrate diffusion gradients that cause the growth of filamentous and finger type structures. To avoid it, non-aerated feeding for the hydrolysis of the particulate substrate is recommended (Pronk *et al.* 2015). Nevertheless, even with non-aerated feeding phases longer than 90 min, the complete hydrolysis is not guaranteed (de Kreuk *et al.* 2010; Wagner *et al.* 2015). In this regard, the inclusion of famine periods during the aeration stage results in a clue variable to promote the formation of stable AGS because it positively influences the granulation process, accelerating the formation of highly-structured and compact aerobic granules (Corsino *et al.* 2017; Sun *et al.* 2021). In general, the duration of the famine phase represents between 65% and 70% of the total cycle length (López-Palau *et al.* 2012; Corsino *et al.* 2017; Sun *et al.* 2021). However, the operation with such a long starvation period reduces the volumetric treatment capacity because of the increase of the HRT. Therefore, it is necessary to identify the minimum famine phase that does not cause filamentous growth or favors the formation of stable AGS to keep a high rate SBR performance.

This work addresses the influence of the duration of the famine phase on the properties of the AGS, as well as the adaptation capability of the biomass to changes in the aeration conditions and in the organic loading rate (OLR) (gradual increases versus OLR shocks). For this purpose, an experiment was designed to compare an abrupt versus a gradual reduction in the famine phase time (t_{fam}) in two SBR of AGS fed with greywater.

METHODS

Experimental setup

Two identical SBR with a height/diameter ratio of 10:2 and working volume of 3.3 L were fed with greywater in a non-aerated mode, from the bottom of the SBR. The effluent was withdrawn through an adjustable port, whose position was fixed above the settled granular sludge bed (Figure 1). The growth of biomass during the experiment changed the height of the settled granular sludge bed, which concomitantly adjusted the position of the withdrawal port to prevent the draining of solids from biomass with the effluent. To avoid an excessive increase in the height of the settled sludge bed, the biomass was periodically purged to maintain exchange volume ratios V_{er} (V_0/V_T) $\geq$0.70.

As a consequence of the adjusted position of the withdrawal port, the length of the filling (t_f), settling (t_s), and withdrawal (t_w) stages, as well as the exchange volume ratio, varied during the experiment. The cycles stages length was fill (t_f) 1.5–3 min, settle (t_s) 9.5–11 min, and withdrawal (t_w) 2–3 min. To modify the value of t_f and t_w, the pump's velocity was adjusted.

To analyze the effect of the reduction of the famine phase over the granular sludge properties, the aeration stage length (t_{ae}) was gradually reduced over 20 weeks in R1 (Runs I to IV), and abruptly reduced from 5.8 to 2.8 h in R2 (Runs I and II). Table 1 shows that the reduction of t_{ae} produced a shortening of the famine phase (t_{ae}–$t_{feast} = t_{fam}$).

The influent used as feed for both SBRs was a greywater mixture from washbasin, shower, kitchen sink, and washing machine. The individual samples were obtained from a household in Mexico City. After the collection, the composite samples

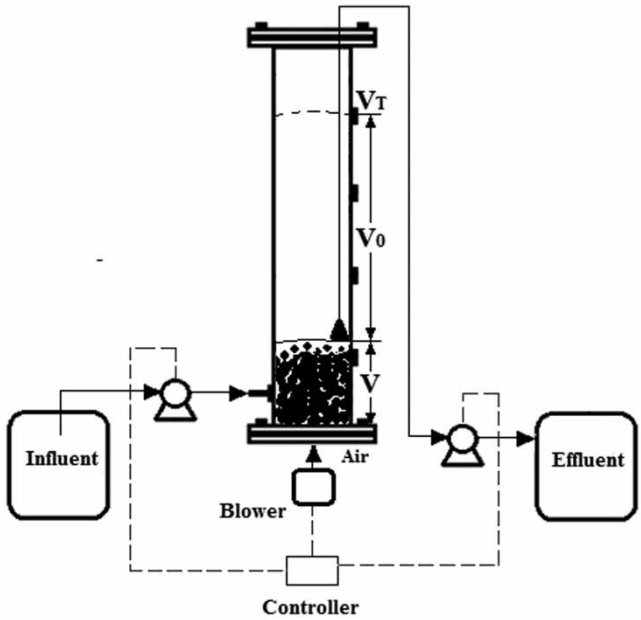

Figure 1 | SBR diagram: V_t = working reactor volume, V = settled granular sludge bed volume, $V_0 = V_t - V$ = exchanged volume.

Table 1 | Characteristics of the operational cycles of both SBR

	R1 and R2	R1			R2
	Run I	Run II	Run III	Run IV	Run II
t_{ae} (h)	5.8	4.6	3.8	2.8	2.8
Average t_{feast} (h)	2.5	2.5	2.5	2.5	2.5
Average t_{fam} (h)	3.3	2.1	1.3	0.3	0.3
Run duration (d)	0–35	36–70	71–105	106–140	36–140

were stored at 5.0 ± 2 °C for its preservation and analysis. Table 2 shows that the physicochemical composition of greywater presented a wide variability during the experimental period due to the natural variation of domestic habits.

Both reactors were inoculated with a sample of mature and stable AGS, previously cultivated in a laboratory-scale SBR with an HRT of 8 h, using greywater from the same household as influent (Rojas-Z *et al.* 2017). The granules presented a rounded-shaped morphology (Figure 4(a)), with a zone settling velocity and SVI of 16.5 m h^{-1} and 67.6 mL g^{-1}, respectively. The mixed liquor suspended solids (MLSS) during the start-up was 1.5 g L^{-1}.

Analytical methods

Total and soluble chemical oxygen demand (COD_t, COD_s), total and volatile suspended solids (TSS, VSS), sludge volume index (SVI), and v_s as zone settling velocity were determined according to Standard Methods (APHA 2012). The biomass disintegration coefficient (δ) was determined stirring a mixed liquor sample at 200 rpm for 5 min and measuring the supernatant solids as TSS (Ghangrekar *et al.* 2005). Granules density (κg) was calculated by the blue dextran method (Beun *et al.* 2002) and the particle size distribution (PSD) by Laguna *et al.* (1999). The extracellular polymeric substances (EPS) was determined by the heating extraction method (Le-Clech *et al.* 2006), in which a mixed liquor sample taken at the end of the cycle was centrifuged at 2,800 *g* for 15 min and filtered with a 0.45 μm pore size membrane. The filtrate was used to determine the not-bound EPS (NB-EPS), and the precipitate was resuspended and heated in water bath at 80 ± °C for 10 min. This sample was centrifuged at 2,800 *g* for 10 min and filtered for tightly-bound EPS (TB-EPS) extraction. The EPS was quantified by the protein (Lowry *et al.* 1951) and carbohydrate concentrations (DuBois *et al.* 1956).

Table 2 | Average composition of the greywater used as influent

	Concentration (mg L^{-1})
COD_T	662 ± 185
COD_s	495 ± 197
CODp	168 ± 81
NH_4^+-N	18.7 ± 17.3
PO_4^{3-}-P	10.5 ± 6.0

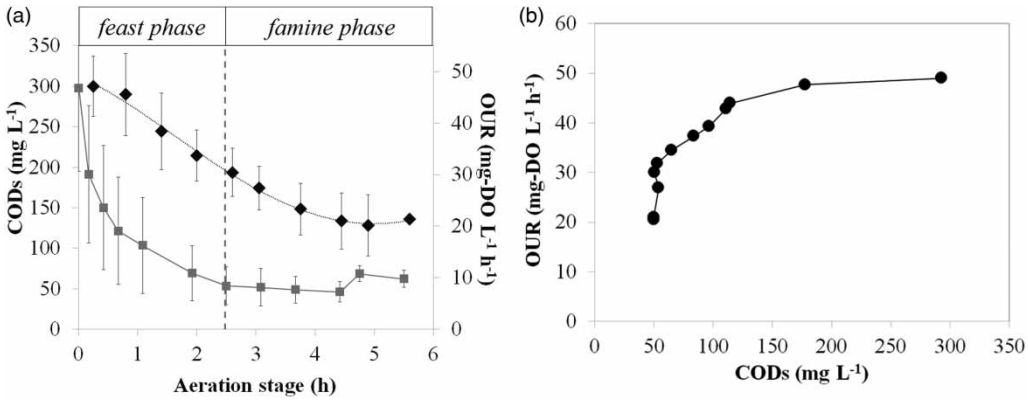

Figure 2 | (a) COD_S soluble consumption (■) and change on the OUR (◆) during the aeration stage, (b) OUR as a function of substrate concentration (COD_s).

The COD removal rate (r_{COD_s}) was evaluated following COD_s consumption in 27 different SBR cycles. Bulk liquid samples were taken from the reactors at time intervals and filtered for COD_s analysis. The AGS OUR was determined by using a fast response dissolved oxygen (DO) meter (WTW, 3410 IDS), for which AGS samples were taken from the SBR and placed in contact with greywater in 600 mL glass vessels, keeping the same substrate to microorganisms ratio (S/X) as in the SBR. The OUR at defined intervals was determined by measuring the DO consumption when the aeration was shut off, in 12 different assays. The beginning of the feast phase was observed when the OUR was no longer COD_s dependent.

AGS morphology and structure were analyzed using a digital cellphone camera and a scanning electron microscope (SEM) (Jeol, JSM-5900 LV). For SEM analysis, granule samples were fixed for 20 h with a 0.35 M glutaraldehyde in phosphate buffer solution (pH = 7.4), and then washed using phosphate buffer and post-fixed with 0.1 M OsO_4 for 2 h. Then they were dehydrated with increasing ethanol concentrations (30, 40, 50, 70, 80, 90, and 100%) in successive steps every 15 min, and to the critical point using a dryer (Tousimis, Sandri 780B). Finally, samples were coated with gold for observation.

RESULTS AND DISCUSSION

Analysis of the aeration stage of the SBR cycles

The feast phase began with the aeration stage of the SBR, in which the readily available substrate was fast removed (Figure 2(a)), inducing high oxygen uptake (OUR = 55 mg-DO L^{-1} h^{-1}) and COD removal rates (r_{COD_s} = 8 ± 2.9 mg L^{-1} h^{-1}). The organic assimilable soluble pollutants of greywater were mostly degraded or adsorbed down to 50 mg-COD_s L^{-1} at an average time of 2.5 ± 0.5 h (t_{feast}), when the OUR dropped with no further COD_s removal. The variation within the feast phase length during the operation, which was reflected on the standard deviation, was due to the natural fluctuation of the pollutants concentration in the greywater used as feed (Table 2), as well as by a possible variation on its biodegradability.

The data showed in Figure 2(a) were fitted to potential models to obtain the trendlines for both profiles, obtaining r^2 values higher than 0.99. The interpolation from the trendlines allowed the relationship between the OUR and COD_s to be determined. As can be observed in Figure 2(b), during the feast stage, the OUR depends on the soluble available

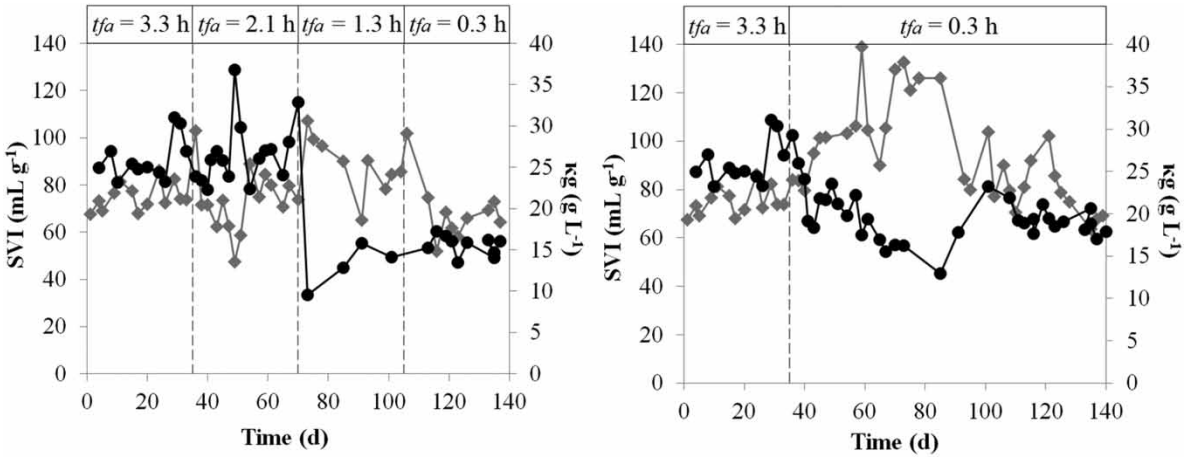

Figure 3 | Evaluation of the SVI (◆) and κg (•) on the granular biomass from R1 and R2.

substrate. Afterwards, when the COD_s reached its minimum (~50 mg-COD_s L^{-1}), the famine phase began, whereas the OUR continued decreasing due to the oxidation of the absorbed substrate during the feast phase (Figure 2(b)). When the absorbed substrate was depleted, the endogenous respiration was reached with a value of ~20 mg-DO L^{-1} h^{-1} after 3.5 h of aeration (Figure 2(a) and 2(b)).

According to kinetic analysis, the feast phase lasted an average of 2.5 ± 0.5 h. Therefore, the famine phase ($t_{fam} = t_{ae}–t_{feast}$) had an average length of 3.3 h during Run I and decreased with the reduction in t_{ae} in the subsequent runs, until it was minimized to 0.3 h in Run IV in the R1 and Run II in the R2, when t_{ae} was 2.8 h in both reactors (Table 1).

Effect of the reduction of the famine phase t_{fam} on the stability of aerobic granules

Figure 3 shows the effect of the t_{fam} reduction on the biomass properties. In R1, the initial reduction of t_{ae} from 5.8 to 4.6 h decreased the t_{fam} from 3.3 to 2.1 h without affecting the properties of the AGS (Figure 3). However, with the subsequent reduction of t_{fam} to 1.3 h (only 34% of t_{ae}), a loss on granular properties was induced, with the SVI increment, and the κg and v_s reduced (Figure 3 and Table 3). A further t_{fam} reduction to 0.3 h resulted in a recovery of the biomass settling properties, with the biomass exhibiting similar SVI and v_s values to those observed with the initial t_{fam} of 3.3 h (Figure 3 and Table 3). In R2, the sudden reduction in t_{fam} from 3.3 to 0.3 h considerably affected the biomass physical properties, increasing SVI and decreasing κg and v_s (Figure 3 and Table 3). Thereafter, from day 90 onwards, the biomass showed a recovery of its properties, with SVI, κg, and v_s reaching 80 mL g^{-1}, 20 g L^{-1}, and 20 m h^{-1}, respectively. This behavior suggests that the reduction on t_{fam} temporarily affects the AGS properties; however, the biomass adapts to the operation with shorter hydraulic conditions.

Results show that filamentous aggregates under short famine conditions can exhibit similar settling properties (v_s and SVI) to those observed in granules operated with long famine periods. However, the κg remained considerably lower and the δ higher (Figure 3 and Table 3), indicating a poor density and structural integrity of the filamentous aggregates formed under short periods, which could affect their stability in the long-term operation. The poor properties of filamentous granules have already been reported by Sharaf *et al.* (2019), who indicates that the filamentous overgrowth affects the stability of the aggregates, even leading to the disruption of their structural integrity, causing their disintegration.

Morphology and structure of AGS

Along with the loss of compactness and settleability, the t_{fam} reduction led to a gradual growth of filamentous organisms on the granular structure. During the application of a $t_{fam} = 3.3$ h, the biomass consisted of granules with the highest sedimentation and compactness properties, with a round-shape morphology (Figure 4(a)). However, the reduction if this variable led to the growth of filamentous microorganisms at the granules surface in both reactors, inducing the formation of highly filamentous aggregates (Figure 4(b)–4(d)). The filamentous outgrowth occurred at a higher rate in R2, where 10 d after the abrupt reduction in t_{fam} was applied, the predominance of filamentous aggregates was observed (Figure 4(e)–4(g)).

Table 3 | Operational conditions and AGS properties during the different experimental periods

	R1 and R2	R1			R2
t_{fam}	3.3 h	2.1 h	1.3 h	0.3 h	0.3 h
Operational conditions					
X (g-MLSS L^{-1})	2.2 ± 0.4	2.9 ± 0.2	1.9 ± 0.5	1.8 ± 0.3	2.1 ± 0.8
Bx (kg-COD kg-VSS^{-1} d^{-1})	1.1 ± 0.4	1.1 ± 0.2	1.6 ± 0.6	2.6 ± 0.6	2.6 ± 1.5
Physical properties					
v_s (m h^{-1})	18.4 ± 1.9	19.1 ± 1.3	16.5 ± 2.3	18.0 ± 4.6	15.8 ± 4.0
δ (%)	0.56	0.81 ± 0.42	0.61 ± 0.60	0.97 ± 0.45	1.21 ± 1.08

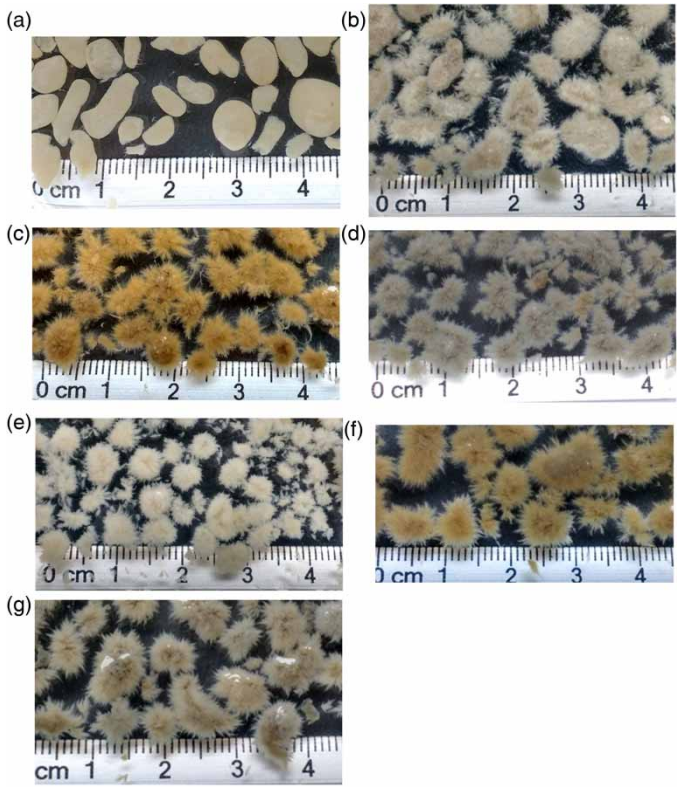

Figure 4 | AGS morphology in R1 (stepwise decrease of t_{ae}) and R2 (abrupt decrease of t_{ae}). (a) R1 and R2, $t_{fam} = 3.3$ h, 24th day. (b) R1, $t_{fam} = 2.1$ h, 68th day. (c) R1, $t_{fam} = 1.3$ h, 105th day. (d) R1, $t_{fam} = 0.3$ h, 119th day. (e) R2, $t_{fam} = 0.3$ h, 68th day. (f) R2, $t_{fam} = 0.3$ h, 105th day. (g) R2, $t_{fam} = 0.3$ h, 119th day.

The analysis of the morphology and structure of the biomass by SEM revealed that the granules at a $t_{fam} = 3.3$ h had a defined surface morphology (Figure 5(a)), with an internal structure integrated by an EPS matrix and bacteria (Figure 5(b)–5(d)). This EPS matrix probably supported the high structural integrity and compactness of the granules during that run (Figure 3 and Table 3). On the other hand, the filamentous granules formed under short length famine conditions in R2 presented a highly porous surface (Figure 5(e) and 5(f)), integrated by filamentous microorganisms (Figure 5(g)), which clustered, forming finger-type structures (Figure 5(f)) similar to those reported by de Kreuk *et al.* (2010). The analysis of its internal structure showed the predominance of different bacteria consortiums (Figure 5(f)), like that of the non-filamentous granules observed during Run I ($t_{fam} = 3.3$ h).

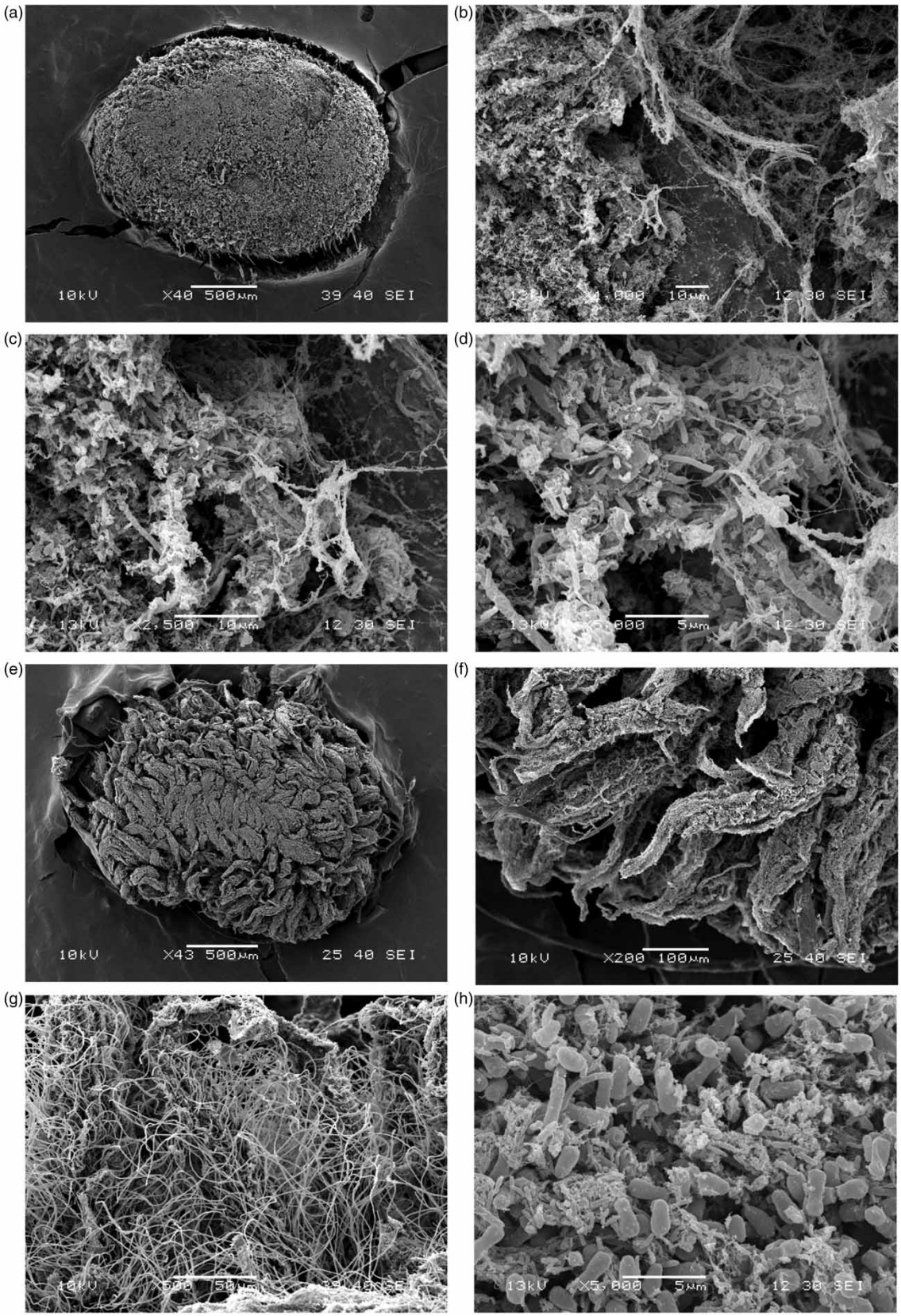

Figure 5 | Structure of AGS at $t_{fam} = 3.3$ h (a–d) and $t_{fam} = 0.3$ h in R2 (e–h).

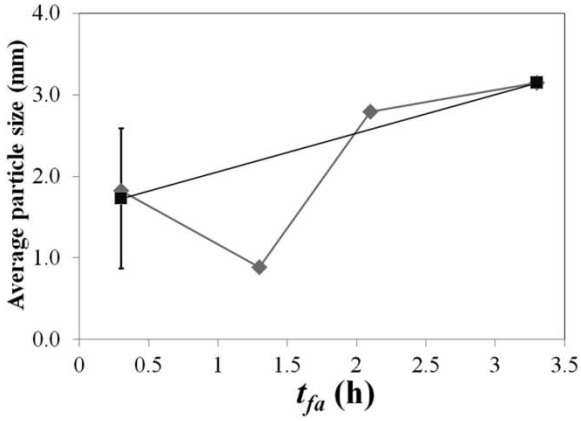

Figure 6 | Change on the average particle size of the AGS with the modification on the t_{fam} in R1 (◆) and R2 (■).

Analysis of the effect of the specific organic loading rate, *Bx,* on AGS PSD and structure

The reduction in t_{ae} resulted in the increase of the specific organic loading rate (*Bx*) (Table 3). Granular biomass showed a good stability at *Bx* between 0.5–1.5 kg-COD kg-VSS^{-1} d^{-1}; however, the application of *Bx* higher than 2.5 kg-COD kg-VSS^{-1} d^{-1} induced organic loading shocks and overstressed conditions that resulted in the partial biomass degranulation on days 108 in R1 and days 40 and 73 in R2.

For both cases, the partial degranulation considerably affected the biomass properties (Figure 3 and Table 3), as well as the PSD (Figure 6). During the operation at $t_{fam} = 3.3$ h, the granular biomass presented an average particle diameter of 3.1 mm. However, after the degranulation in R1, the average particle size decreased to 0.84 mm and the biomass presented a broad size dispersion, with more than 50% of the particles in the range of 0.25–2.8 mm. In R2 the particle size reduced with the application of organic overstressed conditions. However, at the end of the experiment (d140), the biomass was partially recovered from the previous degranulation events while the dispersion was more uniform (50% of particles with diameter = 1.2–2.8 mm).

Overall, it can be inferred that the application of organic overstressed conditions leads to the formation of filamentous aggregates, with a lower diameter than that observed in the stable aerobic granules formed under long famine periods and low organic load rates.

Biomass degranulation and filamentous overgrowth due to the application of high organic loads have already been reported (Pronk *et al.* 2015; Iorhemen & Liu 2021). When the aeration periods are shortened, the specific organic load rate and the feast/famine ratio are increased, producing stressing conditions characterized by a continuous availability of substrate during most of the aeration stage, which favors the selection of the slow growing filamentous microorganisms with high substrate affinity, against floc forming-substrate accumulating bacteria (Liu & Liu 2006). This phenomenon can be potentialized with the use of complex effluents like greywater, in which the initial hydrolysis of the particulate substrate increases the length of the feast phase. If the soluble products from the hydrolysis are consumed in the external area of the granules during the aeration stage, substrate and oxygen diffusion gradients are produced, avoiding the uniform substrate uptake throughout the granular structure (Layer *et al.* 2019). This situation induces the growth of filamentous aggregates, with a porous and weak structure and irregular morphology (Pronk *et al.* 2015), similar to those observed during the application of a $t_{fam} = 0.3$ h for both reactors.

In the current study, the depletion and subsequent recovery on the properties of the biomass indicates that the reduction on t_{ae} initially induces stress conditions which leads to the deterioration of the biomass properties (Table 3). Subsequently, the biomass showed an adaptation reflected on the recovery on their settling properties. This adaptation was associated with a biological selective process, in which those microorganisms presenting high degradation activity under short famine periods were selected. Floc-forming bacteria shows high substrate uptake rates when the concentration in the bulk liquid is high, absorbing the substrate and storing it as reserve during the famine phase (Liu & Liu 2006). Thus, the reduction of the famine periods negatively affects the performance of floc-forming bacteria and favors the proliferation of filamentous microorganisms, which show a high activity under continuous substrate availability conditions.

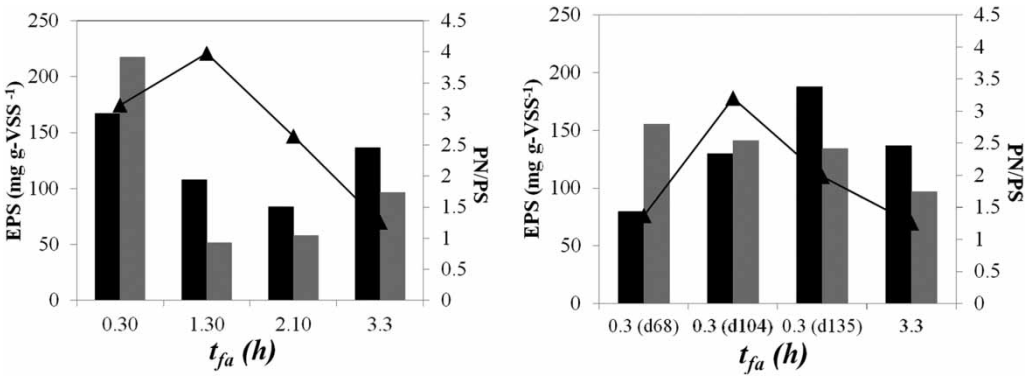

Figure 7 | TB-EPS (■) and NB-EPS (■) content and protein to carbohydrate (PN/PS) ratio (▲) in granular biomass from R1 and R2.

EPS in granular biomass

The EPS content is a factor which define the strength and stability of the granular biomass (Rusanowska *et al.* 2019; Avila *et al.* 2021). EPS tightly bound with cells (TB-EPS) form an inner matrix which provides structural stability to granules. Nonetheless there is a fraction of EPS dissolved in the supernatant (NB-EPS) which are detrimental for the biomass stability and the treatment process performance, by affecting the biomass settleability and the effluent filterability on tertiary treatment units (Le-Clech *et al.* 2006).

In R1 the TB-EPS content of the aerobic granules decreased with the change in t_{fam} from 3.3 to 2.1 h (Figure 7(a)). However, with the subsequent reduction of t_{fam} to 1.3 and 0.3 h, a recovery trend was observed, even exceeding the values of Run I. A similar pattern was observed in R2, where the sudden reduction of t_{fam} to 0.3 h led to the drop in the TB-EPS content (day 68). Afterwards, the recovery of the concentration of TB-EPS was observed (Figure 7(b)) in such a way that the filamentous aggregates at day 135 ($t_{fam} = 0.3$ h) exceeded by 36% the observed values in the AGS at a $t_{fam} = 3.3$ h.

The high TB-EPS content on granules during Run I in R1 and R2 could be the result of the extended famine periods applied ($t_{fam} = 3.3$ h), since microorganisms produce EPS to sustain their metabolism during periods of endogenous respiration (Corsino *et al.* 2017). This high concentration of polymers could have induced the high structural and compaction properties exhibited by the biomass during the longest famine period.

On the other hand, the reduction and subsequent recovery in the TB-EPS content, observed with the shortening of t_{fam}, could be related with the aforementioned adaptation process that resulted on the predominance of filamentous granules. During the transition process of stable-compact granules to filamentous aggregates, the TB-EPS content was considerably reduced. Probably this factor affected the structural stability of the granules, facilitating the partial degranulation when organic overstressed conditions were applied. Thereafter, with the predominance of filamentous aggregates, microorganisms accumulated EPS to keep the stability of the structure. However, in this case, the EPS were not consumed due to the minimization of periods of endogenous respiration. High EPS contents by filamentous microorganisms have been reported by Le-Clech *et al.* (2006).

Regarding the analysis of the NB-EPS, in R1 a decreasing trend in their concentration was observed with the modification on t_{fam} to 2.1 and 1.3 h, but a considerable increase with the further change to 0.3 h (Figure 7(b)). In R2, the sample analyzed on day 68 ($t_{fam} = 0.3$ h) showed an increase of 60% in the NB-EPS concentration with respect to the granular sludge of the first operational run ($t_{fam} = 3.3$ h). This indicates that the filamentous aggregates formed at $t_{fam} = 0.3$ h produced larger NB-EPS than the compact-stable granules, which could be related with the stressing conditions induced by the increasing specific organic loading rate, *Bx*, resulting in EPS being released to the mixed liquor.

The amount of proteins (PN) in the biomass of both reactors was always higher than that of the carbohydrates (PS). A PN/PS > 1 ratio can be interpreted as a positive factor in the structural stability of granular sludge because proteins contribute more to hydrophobicity than carbohydrates, reducing electrostatic repulsions and encouraging the bacterial aggregation (Rusanowska *et al.* 2019). Maybe this factor allowed the formation of new granules after the degranulation induced by organic overstressed conditions.

Overall, the operation with the longest t_{fam} of 3.3 h and low *Bx* promoted the most stable granular biomass with high settling and structural properties, as well with a high TB-EPS content and low NB-EPS concentrations in the supernatant.

CONCLUSIONS

The famine phase reduction allowed shortening of the HRT, increasing the volumetric treatment capacity of the SBR. However, short famine periods induced the deterioration of the physical properties of the biomass due to filamentous outgrowth. The filamentous growth on granular biomass is a progressive process, observed about day 10 when the t_{fam} was abruptly reduced from 3.3 to 0.3 h, and in a longer period about day 45 when the t_{fam} was gradually reduced. This resulted in a loss of compactness and integrity in the biomass of both reactors, manifested in an increase in the SVI and the reduction of the density, settling velocity, and the disintegration coefficient. Biomass properties were especially affected in R1 when the t_{fam} was reduced from 2.1 to 1.3 h, leading to the poorest observed values, whereas in R2, the abrupt reduction on t_{fam} led to the continuous deterioration of the physical properties during the subsequent 45 days. The reduction on t_{fam} led to the application of organic overstressed conditions, which induced the instability in the granular biomass properties and led to the eventual degranulation when the applied Bx was higher than 2.5 kg-COD kg-VSS^{-1} d^{-1}. This phenomenon could be related to steep diffusion gradients induced by the increase in the particulated substrate supply rate. Under this situation, the granular structure is weakened because of the reduction in the EPS content. However, after the degranulation events, the biomass of both reactors exhibited a recovery due to the formation of new small filamentous granules, indicating the adaptation of the biomass to the change in the feast–famine balance conditions.

DATA AVAILABILITY STATEMENT

All relevant data are available from an online repository or repositories (https://drive.google.com/file/d/19VKja3z-jixPfPRQzQlZJmLOFYluE_xM1/view?usp=sharing).

REFERENCES

APHA 2012 *Standard Methods for the Examination of Water and Wastewater*, 22nd edn. American Public Health Association, Washington, DC.

Avila, I., Freedman, D., Johnston, J., Wisdom, B. & McQuarrie, J. 2021 Inducing granulation within a full-scale activated sludge system to improve settling. *Water Sci. Technol.* **84** (2), 302–313. https://doi.org/10.2166/wst.2021.006.

Bajpai, M., Katoch, S. S. & Chaturvedi, N. K. 2019 Comparative study on decentralized treatment technologies for sewage and greywater reuse– A review. *Water Sci. Technol.* **80**, 2091–2106. doi:10.2166/wst.2020.039.

Beun, J. J., Hendriks, A., Loosdrecht, M. C. M. V. A. N., Morgenroth, E., Wilderer, P. A. & Heijnen, J. J. 2002 Aerobic granulation in a sequencing batch. *Water Res.* **36**, 702–712.

Caluwé, M., Dobbeleers, T., D'aes, J., Miele, S., Akkermans, V., Daens, D., Geuens, L., Kiekens, F., Blust, R. & Dries, J. 2017 Formation of aerobic granular sludge during the treatment of petrochemical wastewater. *Bioresour. Technol.* **238**, 559–567. https://doi.org/10.1016/j.biortech.2017.04.068.

Corsino, S. F., di Biase, A., Devlin, T. R., Munz, G., Torregrossa, M. & Oleszkiewicz, J. A. 2017 Effect of extended famine conditions on aerobic granular sludge stability in the treatment of brewery wastewater. *Bioresour. Technol.* **226**, 150–157. https://doi.org/10.1016/j.biortech.2016.12.026.

de Kreuk, M. K., Kishida, N., Tsuneda, S. & van Loosdrecht, M. C. M. 2010 Behavior of polymeric substrates in an aerobic granular sludge system. *Water Res.* **44**, 5929–5938. https://doi.org/10.1016/j.watres.2010.07.033.

DuBois, M., Gilles, K. A., Hamilton, J. K., Rebers, P. A. & Smith, F. 1956 Colorimetric method for determination of sugars and related substances. *Anal. Chem.* **28**, 350–356.

Ghangrekar, M. M., Asolekar, S. R. & Joshi, S. G. 2005 Characteristics of sludge developed under different loading conditions during UASB reactor start-up and granulation. *Water Res.* **39**, 1123–1133. https://doi.org/10.1016/j.watres.2004.12.018.

Iorhemen, O. T. & Liu, Y. 2021 Effect of feeding strategy and organic loading rate on the formation and stability of aerobic granular sludge. *J. Water Process Eng.* **39**. https://doi.org/10.1016/j.jwpe.2020.101709.

Laguna, A., Ouattara, A., Gonzalez, R. O., Baron, O., Fama, G., El Mamouni, R., Guiott, S., Monroy, O. & Macarie, H. 1999 A simple and low cost technique. *Water Sci. Technol.* **40**, 1–8.

Layer, M., Adler, A., Reynaert, E., Hernandez, A., Pagni, M., Morgenroth, E., Holliger, C. & Derlon, N. 2019 Organic substrate diffusibility governs microbial community composition, nutrient removal performance and kinetics of granulation of aerobic granular sludge. *Water Res.* **4**, 100033. https://doi.org/10.1016/j.wroa.2019.100033

Le-Clech, P., Chen, V. & Fane, T. A. G. 2006 Fouling in membrane bioreactors used in wastewater treatment. *J. Memb. Sci.* **284**, 17–53. https://doi.org/10.1016/j.memsci.2006.08.019.

Liu, Y. & Liu, Q. S. 2006 Causes and control of filamentous growth in aerobic granular sludge sequencing batch reactors. *Biotechnol. Adv.* **24**, 115–127. https://doi.org/10.1016/j.biotechadv.2005.08.001.

López-Palau, S., Pinto, A., Basset, N., Dosta, J. & Mata-Álvarez, J. 2012 ORP slope and feast–famine strategy as the basis of the control of a granular sequencing batch reactor treating winery wastewater. *Biochem. Eng. J.* **60**, 120–1298. http://dx.doi.org/10.1016/j.bej.2012.08.002.

Lowry, O. H., Rosebrough, N. J., Farr, A. L. & Randall, R. J. 1951 The folin by oliver. *J. Biol. Chem.* **193**, 265–275. https://doi.org/10.1016/0304-3894(92)87011-4.

Pronk, M., Abbas, B., Al-zuhairy, S. H. K., Kraan, R., Kleerebezem, R. & van Loosdrecht, M. C. M. 2015 Effect and behaviour of different substrates in relation to the formation of aerobic granular sludge. *Appl. Microbiol. Biotechnol.* **99**, 5257–5268. https://doi.org/10.1007/s00253-014-6358-3.

Qi, K., Li, Z., Zhang, C., Tan, X., Wan, C., Liu, X., Wang, L. & Lee, D.-J. 2020 Biodegradation of real industrial wastewater containing ethylene glycol by using aerobic granular sludge in a continuous-flow reactor: performance and resistance mechanism. *Biochem. Eng. J.* **161**, 107711.

Rojas-Z, U., Fajardo-O, C., Moreno-Andrade, I. & Monroy, O. 2017 Greywater treatment in an aerobic SBR: sludge structure and kinetics. *Water Sci. Technol.* **76**, 1535–1544. https://doi.org/10.2166/wst.2017.341.

Rusanowska, P., Cydzik-Kwiatkowska, A., Świątczak, P. & Wojnowska-Baryła, I. 2019 Changes in extracellular polymeric substances (EPS) content and composition in aerobic granule size-fractions during reactor cycles at different organic loads. *Bioresour. Technol.* **272**, 188–193. https://doi.org/10.1016/j.biortech.2018.10.022.

Sengar, A., Basheer, F., Aziz, A. & Farooqi, I. H. 2018 Aerobic granulation technology: laboratory studies to full scale practices. *J. Cleaner Prod.* **197**, 616–632. doi:10.1016/j.jclepro.2018.06.167.

Sharaf, A., Guo, B. & Liu, Y. 2019 Impact of the filamentous fungi overgrowth on the aerobic granular sludge process. *Bioresour. Technol. Rep.* **7**. https://doi.org/10.1016/j.biteb.2019.100272.

Sun, Y., Gomeiz, A. T., Van Aken, B., Angelotti, B., Brooks, M. & Wang, Z.-W. 2021 Dynamic response of aerobic granular sludge to feast and famine conditions in plug flow reactors fed with real domestic wastewater. *Sci. Total Environ.* **758**, 144155. https://doi.org/10.1016/j.scitotenv.2020.144155.

Wagner, J., Weissbrodt, D. G., Manguin, V., Ribeiro da Costa, R. H., Morgenroth, E. & Derlon, N. 2015 Effect of particulate organic substrate on aerobic granulation and operating conditions of sequencing batch reactors. *Water Res.* **85**, 158–166. https://doi.org/10.1016/j.watres.2015.08.030.

Wang, X., Chen, Z., Shen, J., Kang, J., Zhang, X., Li, J. & Zhao, X. 2020 Effect of carbon source on pollutant removal and microbial community dynamics in treatment of swine wastewater containing antibiotics by aerobic granular sludge. *Chemosphere.* **260**, 127544. https://doi.org/10.1016/j.chemosphere.2020.127544.

Yuan, Q., Gong, H., Xi, H., Xu, H., Jin, Z., Ali, N. & Wang, K. 2019 Strategies to improve aerobic granular sludge stability and nitrogen removal based on feeding mode and substrate. *J. Environ. Sci.* **84**, 144–154.

First received 9 March 2021; accepted in revised form 28 June 2021. Available online 14 July 2021